Variation of the Frost Boundary below Road and Railway Embankments in Permafrost Regions in Response to Solar Irradiation and Winds

N.I. Kömle[1] and Wenjie Feng[2]
[1)] Space Research Institute, Austrian Academy of Sciences, Graz, Austria
[2)] State Key Laboratory of Frozen Soil Engineering, CAREERI, CAS, Lanzhou, China

*Corresponding author: N.I. Kömle, Space Research Institute, Austrian Academy of Sciences, Schmiedlstrasse 6, A-8042 Graz; Austria. Email: norbert.koemle@oeaw.ac.at

Abstract: We present COMSOL solutions for a coupled gas flow and heat transfer problem, which occurs particularly when traffic pathways are constructed in high altitude and arctic regions, where the underground is frozen soil. To avoid melting of the frozen ground (which usually leads to mechanical instability) one has to find suitable measures to keep the subsurface soil and the embankment suitably cool. Here we study two ways to do this: (i) protection of the embankment by awning constructions against unwanted heating by solar irradiation and (ii) cooling or heating by lateral gas flows, e.g. natural winds. To study these effects experimentally, a lab–setup has been established at CAREERI, Lanzhou, which allows to simulate both the solar irradiation and the winds. The COMSOL model presented in this paper mimics this laboratory setup and can therefore be used as a numerical tool to predict and interpret the experimental results. We calculate the flow field and its influence on the temperature field in the embankment and the subsurface soil for laminar flows, using the appropriate COMSOL application modes.

Keywords: Railway embankments, awnings, permafrost regions.

1. Introduction

In arctic and high altitude regions, as for example the Qinghai–Tibet high plateau in China, engineers dealing with the construction of road and railway routes are frequently faced with the problem that the natural ground is permanently frozen even in the summer season. This can cause serious problems for the safety of traffic routes, because the traffic load usually creates additional heat leading to uncontrolled melting of the soil. Together with natural sources as solar irradiation and temperate winds, serious damage can occur. An example is shown in Figure 1. Therefore it is very important for the planning of any new infrastructure project in these sensitive areas to predict the variation of the frost isotherm in response to various heat sources and surface winds. It will become even more important in the future, since due to the global warming trend of the world's climate gradual melting of the permafrost is observed in arctic and high altitude regions (Wu et al., 2008). For road construction engineers this means that they have to find ways to protect the permafrost below the embankment as good as possible by shielding the ground from unnecessary heat input. One way to do this is to use “awnings" along the embankments, which keep radiation off and channel cold winds near the ground. At the CAREERI soil laboratory an experimental setup has been established, where irradiation of a road embankment as well as air flow with a controlled temperature can be simulated. This allows to study the reaction of the frozen soil and embankment to a given radiation level and air flow, both for unprotected embankments and for embankments shielded by awning constructions. Compared to observations in the natural field environment, this allows to vary parameters in a more controlled way. Since there is a strong interaction between heat transfer and the hydrodynamic gas flow in this problem, numerical modeling is an important tool both for the preparation of such indoor tests and for their evaluation. Previous work in this field, focusing on the effect of awnings in road construction work and on the thermal conductivity of road

Figure 1. Example of the damage of a road embankment in the high altitude Qinghai-Tibet region due to uncontrolled permafrost melting (source: *http://nsidc.org/frozenground/people.html*).

construction materials have been published in the recent years (Feng et al., 2006; Kömle et al., 2007; Kömle et al., 2008). They form the basis for the parameter values used in this report.

2. Problem Formulation

Figure 2 shows the basic setup of the experiment, indicating also the main dimensions. The lower part is the solid domain, representing the natural clay soil and two layers of the road embankment. On the upper left boundary air with a defined temperature (either colder or warmer than the original soil temperature) enters the domain with a given velocity. The upper right side is the free outflow boundary for the air. Inside the air domain a lamp (solid domain) is positioned, which forms an obstacle in the air flow. Radiation is directed only downwards, the backside of the lamp is assumed to be thermally isolated. In the setup with awning the awning construction is positioned 25 cm above the soil. The flow is assumed to be laminar, therefore only low inflow velocities (of the order of cm/s, i.e. slow winds) can be used in the following model implementation.

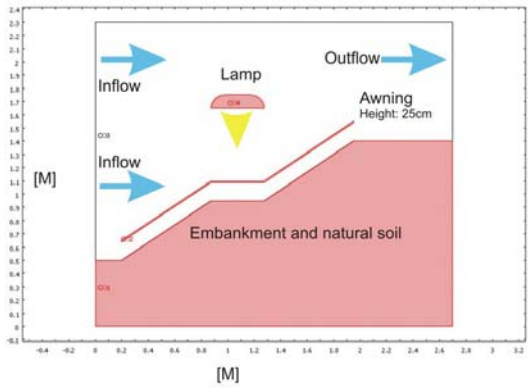

Figure 2: Schematics of the experimental setup in the soil laboratory and its implementation in the COMSOL model geometry. The geometry used for the models without awning are the same, but without the part representing the awning.

To solve the problem described above, the gas flow must be combined with the heat transfer. For this purpose we use the *Weakly Compressible Navier-Stokes Equations* in their quasi-stationary form

$$\rho u \cdot \nabla u = \left[-pI + \eta\left(\nabla u + (\nabla u)^T\right) - \left(\frac{2\eta}{3} - \kappa\right)(\nabla u) I \right]$$

$$\nabla \cdot (\rho u) = 0$$

and couple them with the time–dependent heat transfer equation which has the form

$$\rho C \frac{\partial T}{\partial t} + \nabla \cdot (-k \nabla T) = Q - \rho C u \cdot \nabla T$$

2. COMSOL Implementation

These equations are implemented in COMSOL as a Multiphysics problem using the *Weakly Compressible Navier–Stokes* application mode and the *General Heat Transfer* application mode. The physical parameters used for the different domains (solid and fluid as shown in Figure 2) are listed in Table 1. Hereby it has to be kept in mind that the thermal–related material parameters (ρ, C_p, k) change with time when the frozen soil melts or the warm soil freezes. To allow for this variation we implement step functions depending on the actual local temperature and the melt temperature T_m as follows:

$$\rho_{clay} = \frac{1}{2}\left(\rho_{clayf} + \rho_{clayu}\right) + \left(\rho_{clayu} - \rho_{clayf}\right)\frac{1}{\pi} \cdot \arctan\left[b_m (T - T_m)\right]$$

$$C_{clay} = \frac{1}{2}\left(C_{clayf} + C_{clayu}\right) + \left(C_{clayu} - C_{clayf}\right)\frac{1}{\pi} \cdot \arctan\left[b_m (T - T_m)\right]$$

$$k_{clay} = \frac{1}{2}\left(k_{clayf} + k_{clayu}\right) + \left(k_{clayu} - k_{clayf}\right)\frac{1}{\pi} \cdot \arctan\left[b_m (T - T_m)\right]$$

In order to implement the possibility of melting and freezing of the soil and to allow the correct inclusion of the melting/freezing heat, one has to modify the soil's thermal capacity accordingly as:

$$C = C_{clay} + D_m Q_m$$

Hereby $D_m(T)$ is a narrow Gauss function around the melting temperature T_m, which ensures that melting or freezing heat is only released or consumed when the material is close to $T = T_m$. This is an analytical approximation of a Dirac-Delta function around the point $T = T_m$:

$$D_m = \frac{e^{-(T-T_m)^2/\sigma^2}}{\sqrt{\pi\sigma^2}}$$

To obtain a convergent solution with COMSOL, the problem has to be solved in several steps.

First, a stationary solution for the gas flow across the embankment is calculated, where no heating or cooling of the inflowing air and no radiative heating by the lamps is assumed. This solution results in a stationary flow field for the gas across the embankment. Using the *Stationary Segregated Solver* (on the *Solver Parameters* page) results in a convergent solution, where the temperature remains constant throughout. Convergence is, however, only reached for low wind velocities which guarantee largely laminar flow conditions. In our example we used a parabolic velocity profile at the inflow boundary according to the formula

$$u(y) = u_{\max}\left[1-\left(\frac{y-y_m}{y_{top}-y_m}\right)^2\right]$$

with

$$y_m = \frac{1}{2}\left(y_{bottom}+y_{top}\right)$$

Here u_{max} is the maximum inflow velocity at the position y_m and y_{bottom} and y_{top} are the lower and upper limits of the inflow region. There $u = 0$ because of the no-slip boundary condition for the gas flow along solid/gas boundaries. In the example shown here $u_{max} = 0.05$ m/s was chosen.

In the second step, the stationary solution obtained as a result of Step 1 is used as the start solution for a time–dependent calculation: at t = 0 s warmer or colder air starts to flow into the domain from the left boundary and subsequently interacts with the solid embankment and the top boundary ("ceiling" of the lab–setup). In this case the time-dependent segregated solver is used. The time–dependent calculation is executed over a period of 60 s. To provide smooth boundary conditions for the heating or cooling of the gas at the inflow boundary we use the following algebraic function of t:

$$T_{bound} = T_{init} + \Delta T \cdot \frac{\arctan\left[b_1(t-t_1)\right]\cdot\arctan\left[-b_2(t-t_2)\right]+\pi^2/4}{\arctan\left[b_1(t_2-t_1)/2\right]\cdot\arctan\left[-b_2(t_1-t_2)/2\right]+\pi^2/4}$$

Choosing appropriate values of b_1, b_2 results in a smooth, but still reasonably sharp temperature variation at the inflow boundary. The temperature change takes place at time t_1 and t_2, respectively. In our example t_2 is beyond the time-dependent calculation limit, i.e. there is only one temperature step within the calculation time (either heating or cooling, depending on the sign of ΔT).

In the third step, the obtained solution after t = 60 s is used as the start solution for a long term calculation: The lamp above the embankment is switched on and radiates with a power of 2200 W towards the embankment surfaces. The lower side of the lamp is considered as an IR-radiator, which can both emit and receive infrared radiation, while the backside of the lamp remains thermally isolated. The heating of the embankment by the emitted radiation is implemented by modifying the concerned internal boundaries. In the *Boundary Settings* menu they are changed from *Continuity* into *Heat Source/Sink* which allows to activate the *Surface-to-Surface* radiation mode with appropriate emissivity values. This long term calculation is run over 2 days (48 hours) and saved every 900 s (15 min).

4. Results

The following figures show the results of some illustrative model calculations performed along the lines described above. The parameter values and constants used in the model calculations are listed in Table 1.

In order to evaluate the influence of the gas flow temperature on the motion of the melting isotherm we have computed two cases. First, a gas stream 10 K warmer than the initial overall temperature of the system flows across the surface and heats it in addition to the lamp radiation. In the second case, the gas stream moving across the surface is 10 K colder than the initial overall temperature. Figure 3 shows the gas flow of the heated air across the domain in

the first 60 seconds for the case without awning, in Figure 4 the same case including the awning is shown. The white arrows indicate the flow field, note the shadow zones with low velocities that develop behind the lamp and on the road plateau. In Figure 4 the channeled flow between the awning and the embankment can also be seen.

The following figures show the influence of the irradiation for the *no awning* and the *awning* cases, respectively. The awning structure is assumed to have a high IR–emissivity on the upper side and a low emissivity on the lower side, which is directed towards the soil. This would maximize the protection effect for the frozen soil and can be realized by appropriate coatings of the awning surfaces. For the soil and the lamp, which radiate against each other, the same emissivity values are used in the *awning* and the *no awning* case, respectively.

The development of the melting isotherm in response to the irradiation by the lamp with 2200 W over a period of 48 hours is shown for four different cases in the following figures:

Figure 5: no awning – heated air
Figure 6: awning – heated air
Figure 7: no awning – cooled air
Figure 8: awning – cooled air

In all figures the white line indicates the 0°C isotherm, which – in the solid domain – represents the melt/freeze boundary.

Parameter	**Value**	**Description**
k_{clayu}	1.60 [W/m/K]	soil heat conductivity (unfrozen)
k_{clayf}	1.98[W/m/K]	soil heat conductivity (frozen)
ρ_{clayu}	1800 [kg/m^3]	soil density (unfrozen)
ρ_{clayf}	1800 [kg/m^3]	soil density (frozen)
C_{clayu}	1266 [J/kg/K]	soil heat capacity (unfrozen)
C_{clayf}	977.2 [J/kg/K]	soil heat capacity (frozen)
k_{air}	0.024[W/m/K]	air heat conductivity
varrho_{air}	1.169[kg/m^3]	air density
C_{air}	1005[J/kg/K]	air heat capacity
η	17.2e-6[Pa s]	air viscosity
T_{init}	273.15 [K]-5[K]	initial temperature
p_0	1e5[Pa]	air pressure
T_m	273.15[K]	ice melting temperature
b_m	10[1/K]	sharpness parameter for phase change
σ	0.1[K]	Gauss parameter for phase change
b_1	10[1/s]	sharpness parameter for lamp on
b_2	10[1/s]	sharpness parameter for lamp off
ΔT	± 10[K]	air temperature change
watercontent	0.12	water content of soil
Q_{mH2O}	333e3[J/kg]	ice melting heat
Q_m	watercontent* Q_{mH2O}	soil melting heat
k_{awning}	238[W/m/K]	awning thermal conductivity
ρ_{awning}	2700[kg/m^3]	awning density
C_{awning}	945[J/kg/K]	awning heat capacity
k_{lamp}	238[W/m/K]	lamp heat conductivity
ρ_{lamp}	2700[kg/m^3]	lamp density
C_{lamp}	945[J/kg/K]	lamp heat capacity
ε_{lamp}	1.00	lamp emissivity
ε_{clay}	0.75	soil emissivity
$\varepsilon_{awningt}$	0.80	awning top emissivity
$\varepsilon_{awningb}$	0.30	awning bottom emissivity

Table 1: Parameters used in the model.

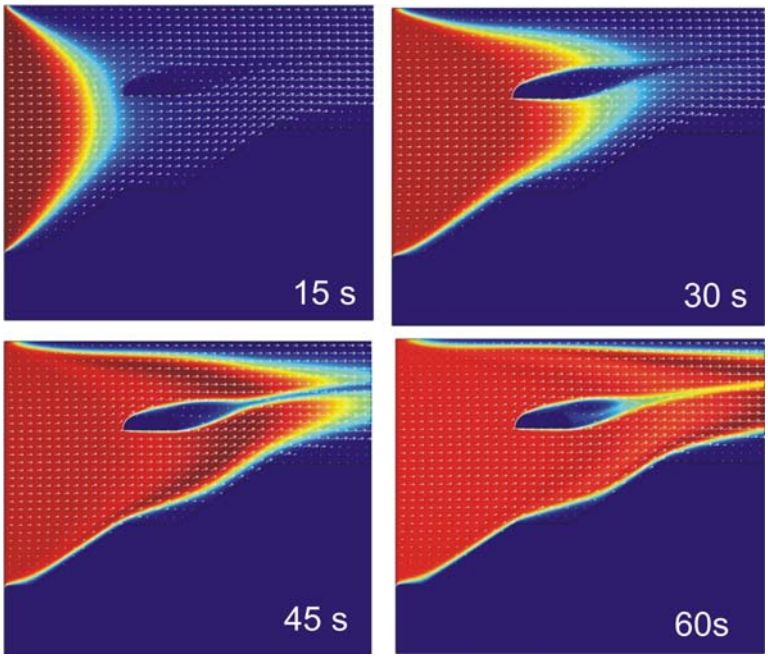

Figure 3: Model results showing the inflow of warm air at the left boundary into the gas domain within the first 60 seconds after the begin of the warm gas inflow.

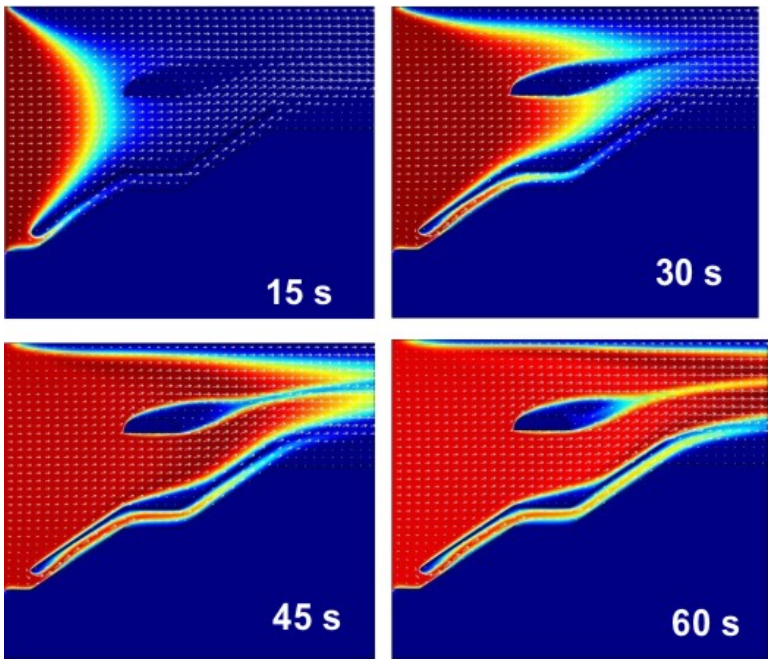

Figure 4: Model results showing the inflow of cold air at the left boundary into the gas domain within the first 60 seconds after the begin of the cold gas inflow.

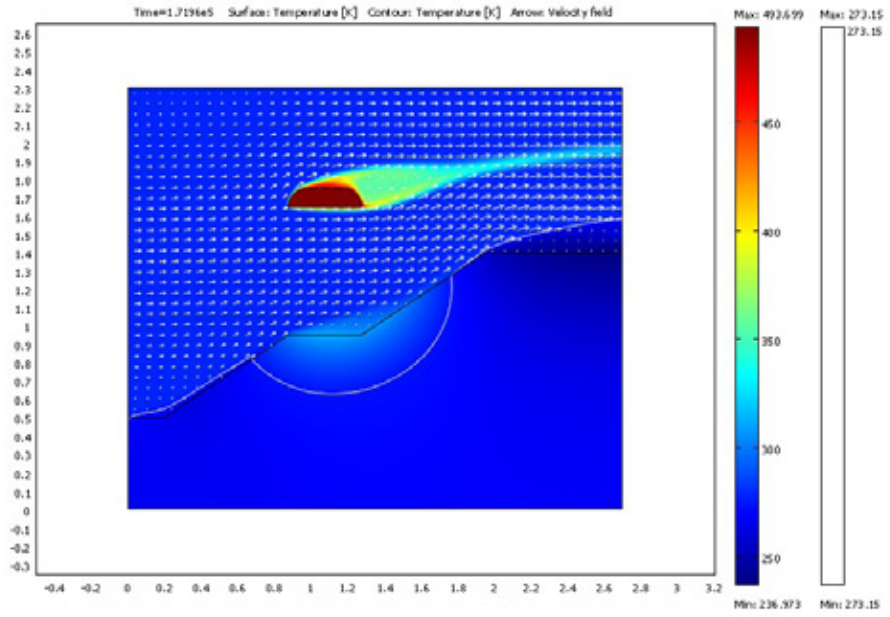

Figure 5: Model result for the long term calculation, 48 hours after the begin of the irradiation by the lamp, when the embankment is not covered by the awning structure. The white line in the solid part (embankment) represents the melting isotherm – warm air case.

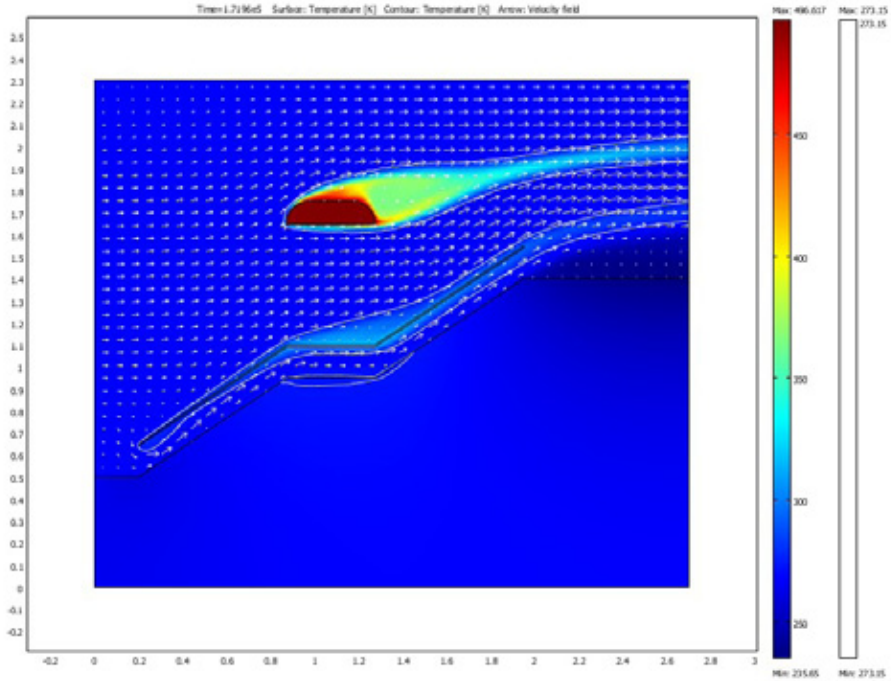

Figure 6: Model result for the long term calculation, 48 hours after the begin of the irradiation by the lamp, when the embankment is covered by the awning structure. The white line in the solid part (embankment) represents the melting isotherm – warm air case.

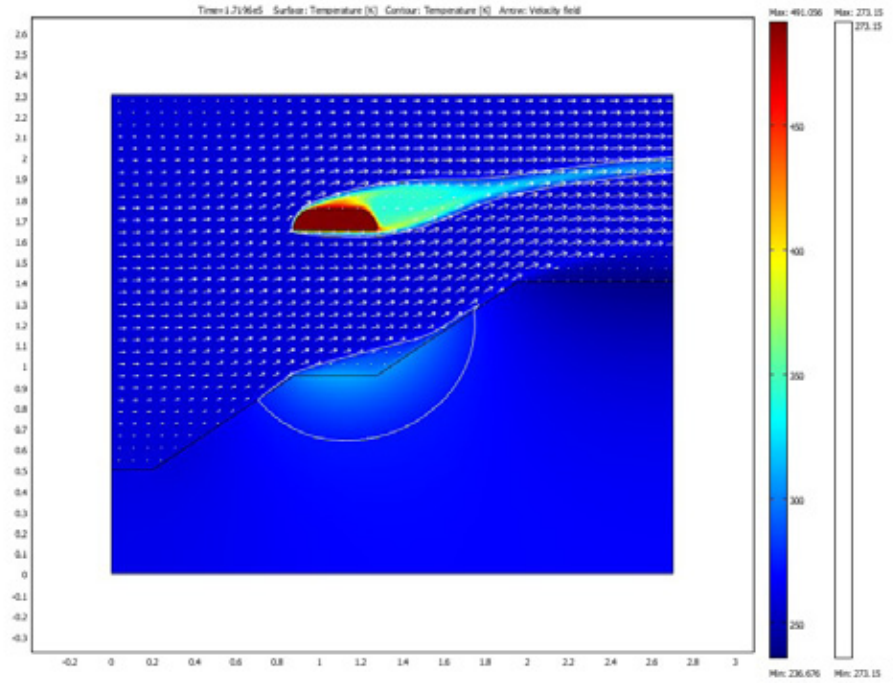

Figure 7: Model result for the long term calculation, 48 hours after the begin of the irradiation by the lamp, when the embankment is not covered by the awning structure. The white line in the solid part (embankment) represents the melting isotherm – cold air case.

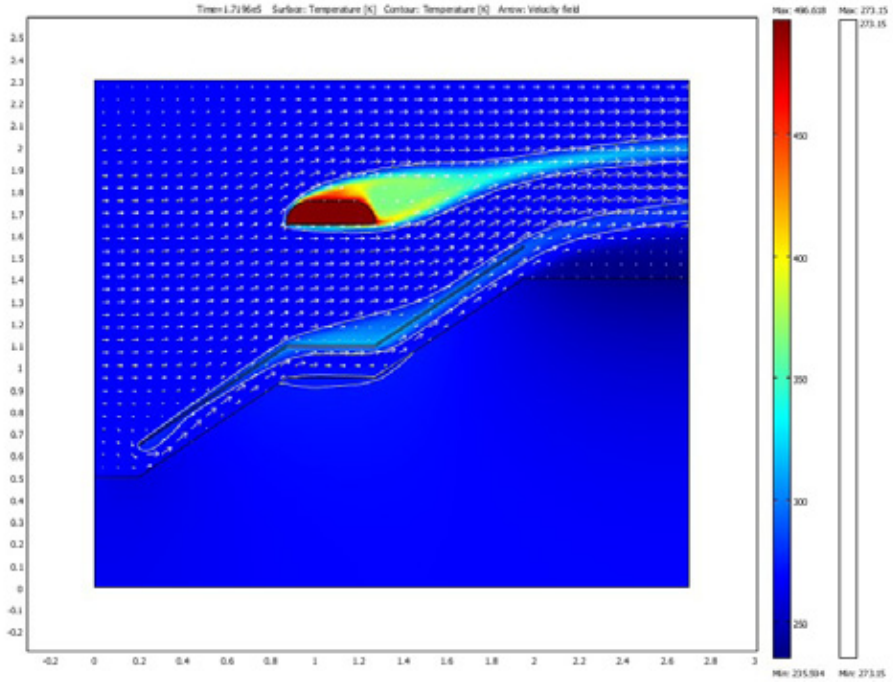

Figure 8: Model result for the long term calculation, 48 hours after the begin of the irradiation by the lamp, when the embankment is covered by the awning structure. The white line in the solid part (embankment) represents the melting isotherm – cold air case.

5. Discussion and Conclusions

Comparison of the *awning* and *no awning* cases indicates that in the latter the frozen ground has retreated considerably farther. For no awning protection the soil below the lamp has melted over about 30 cm depth, while in the awning cases the ground remains frozen below about 5 cm depth, even after 48 hours of constant irradiation. This is due to the protection effect of the awning against the lamp radiation.

On the other hand, the variation of the air temperature has very little influence on the position of the melt boundary after 48 h of irradiation by the lamps. In the no awning case the depth difference is a few millimetres, in the awning case it is even smaller and practically not discernable on the figures.

The models presented can give valuable guidelines for the design of the awning protections, although several aspects have not yet been included. First we have assumed that the irradiation comes from an IR source, therefore only the emissivities of the surfaces enter the model, but not optical parameters like the albedo. When studying irradiation by the sun, this aspect should be included in order to evaluate the influence of albedo variations. Second, the models presented include only laminar gas flow across the embankment, and therefore are restricted to low wind velocities. We tried to build similar models for the turbulent flow cases, but did not succeed to make them produce converging solutions till now, when using the available COMSOL application modes for turbulent gas flow.

Our main conclusion from the presented calculations is that at these low flow speeds the temperature of the air flowing across the embankment has very little influence on the depth of the melting isotherm in the soil and the use of awnings can be very effective in avoiding frost melt. However, one should keep in mind that this picture may change when high velocity, turbulent winds are studied, which can easily occur in the high altitude regions of the Qinghai–Tibet plateau.

6. References

Kömle N.I., Bing H., Feng W.J., Wawrzaszek R., Hütter E.S., He Ping, Marczewski W., Dabrowski B., Schröer K., Spohn T.: Thermal conductivity measurements of road construction materials in frozen and unfrozen state. *Acta Geotechnica* 2, 127–138 (2007).
DOI 10.1007/s11440-007-0032-1.

Kömle N.I., Hütter E.S., Kargl G., Ju H.H., Gao Y., Grygorczuk J.: Development of thermal sensors and drilling systems for application on lunar lander missions. *Earth Moon Planet* **103**, 119–141 (2008).
DOI 10.1007/s11038-008-9240-4 (open access).

Feng Wenjie, Ma Wei, Li Dongqing, Zhang Luxin: Application of awning to roadway engineering on the Quinghai–Tibet plateau. *Cold Regions Science and Technology* **45**, 51–58 (2006).

Wu Qingbai, Cheng Guodong, Ma Wei, Liu Yongzhi: Railway construction techniques adapting to climate warming in permafrost regions. *Advances in Climate Change Research* **4** (Suppl.), 60–66 (2008).

7. Acknowledgements

This work was supported in part by the Austrian *Fonds zur Förderung der wissenschaftlichen Forschung* under project L317–N14.